Angle-resolved photoemission from valence bands of Cu and Au single crystals using 32–200-eV synchrotron radiation*

J. Stöhr, G. Apai, P. S. Wehner, F. R. McFeely, R. S. Williams, and D. A. Shirley

Materials and Molecular Research Division, Lawrence Berkeley Laboratory
and Department of Chemistry, University of California, Berkeley, California 94720

(Received 14 June 1976)

The directional anisotropy in photoemission from valence bands of Cu and Au single crystals has been studied in the photon energy ranges $32 \le h\nu \le 200$ eV, and $32 \le h\nu \le 130$ eV, respectively. Angle-resolved photoemission energy distributions were obtained for electrons emitted in the [001] and [111] directions. Dramatic differences were found between the two directions and strong variations with energy were obtained over the entire energy range. The results are discussed in terms of final-state band-structure effects and/versus strong inelastic damping in the final state. For Cu, spectra taken at $h\nu = 90$ eV along the same symmetry directions at high (90°) and low (35°) take-off angles from the surface show a pronounced narrowing of the d band at low take-off angles. This is attributed to a preferential sampling of the local density of states at the surface by using an appropriate photon energy and take-off angle. The energy dependence of the Au $5d$ intensity has been measured and is found to decrease by a factor of ~ 50 over the investigated photon energy range 40–190 eV.

I. INTRODUCTION

Angle-resolved photoemission (ARP) from single crystals has previously been reported in the ultraviolet (UPS)[1] and x-ray (XPS)[2,3] photoemission ranges. In the two regimes significantly different information is contained in the experimentally observed photoelectron energy distributions (PED's). At UPS energies the PED's obtained by exciting valence electrons are determined by the details of both the initial- (valence-band) and final- (conduction-band) state energies and wave functions.[4,5] In this regime the three-step model of photoemission[5] including strict momentum and energy conservation during the excitation process, has proven to describe the experimental situation quite well. On the other hand, angle-resolved PED's observed at XPS energies basically depend only on the symmetry properties of the initial states.[3] In this case momentum- and energy-conservation selection rules are also important but they are more easily satisfied. Thus final-state band-structure effects are weak. The experimental spectra are well described by the initial density of states modulated by an angle-dependent matrix element.[3]

So far, no ARP studies have been performed in the transition region between UPS and XPS, namely, in the region $40 \lesssim h\nu \lesssim 1000$ eV. Here we report such experiments. We have utilized the first six 8-hr shifts dedicated to synchrotron radiation on the SPEAR storage ring at the Stanford Synchrotron Radiation Project (SSRP).[6] The high-photon flux emitted by SPEAR, which operated at beam currents up to 80 mA,[7] allowed ARP studies of the valence bands (VB) of Cu ($3d$) and Au ($5d$) single crystals in the energy range up to 280 eV for Cu

and 130 eV for Au.

ARP experiments in the photon energy range studied here are of considerable interest because of their high surface sensitivity which arises from a minimum in the photoelectron mean free path in the kinetic energy region around 100 eV.[8] In this range of electron energies the mean free path becomes comparable with the interatomic distance in the solid, and the photocurrent arises largely from the top layers.[1] The theoretical description of the PED's in this range of "strong damping" is a difficult problem. Not only does one have to consider the local states of the outermost surface layer in addition to the bulk states as possible initial states, but the photoemission process *per se* can no longer be described by a simple model because the steps of excitation, transport, and emission are inextricably mixed.[9] It has been argued that because of strong inelastic electron scattering effects the observed spectra might even have to be interpreted in terms of many-body effects rather than single-particle properties like densities of states.[1]

This paper is intended to elucidate some of the above problems by providing the first experimental ARP results in this interesting energy range. It is apparent that ARP studies provide considerably more detailed information than the previously available angle-integrated results.[5,10–12] Experimental details and results are presented in Secs. II and III, respectively. In Sec. IV we discuss the basic physical reasons for an energy and angular dependence of photoemission in the UPS-XPS transitions region. The experimental results for Cu and Au are discussed in these terms in Sec. V. In the concluding Sec. VI we discuss the basic

information obtained from the present investiga-
tion and point out some of the problems stimu-
lated by it.

II. EXPERIMENTS

The experimental geometry is shown in Fig. 1.
The monochromatic[13] photon beam was incident
on a Cu or Au single crystal which was positioned
at the focal point of a cylindrical mirror analyzer
(CMA) modified for ARP studies as discussed be-
low. The electric field vector $\vec{E}$ of the incident
radiation lay in the plane defined by the beam and
the propagation direction of electrons accepted by
the analyzer. Its orientation with respect to the
crystalline axes is shown in Fig. 2. We have
chosen the fourfold cubic axes [100], [010], and
[001] as our frame of reference (x, y, z) and we
describe the spacial orientation of the $\vec{E}$ vector
and the detector in terms of polar (θ) and azimuth-
al (ϕ) angles. The positions of the x-ray beam
and the detector were fixed relative to each other
with the x-ray Poynting vector, $\vec{E}$ vector, and
the detector acceptance axis lying in the horizontal
plane.

The sample holder could be rotated about a ver-
tical axis. Two crystals with a (001) and (111) face,
respectively, were mounted simultaneously on the

sample holder. By raising or lowering the sample
holder the electrons were collected either along
the [001] direction of the (001) crystal or along
the [111] direction of the (111) crystal (cf. Fig. 2).
For Cu it was possible to look at photoelectrons
emitted along both the [001] and [111] axes of the
same crystal by rotating about the vertical axis.
The faces of the crystals were polished to 1 μm
smoothness and then etched before introduction
into the ultrahigh-vacuum (~1 × 10⁻¹⁰-Torr) cham-
ber. The surfaces were then cleaned by argon ion
bombardment and annealed by heating with an elec-
tron gun to remove surface damage.

The CMA, operated in the retarding mode,[14] was
adapted for angle-resolved measurements by plac-
ing a stainless-steel shield with a 11° slit aperture
on the front of the analyzer.[15] The geometrical ar-
rangement of the slit is shown in Fig. 1(b). The ef-
fective acceptance area of the CMA is defined by
the ±6° acceptance width of the CMA[16] and by the
±5.5° slit width of the shield yielding an angular
resolution of ±6° in the horizontal and ~±4° in the
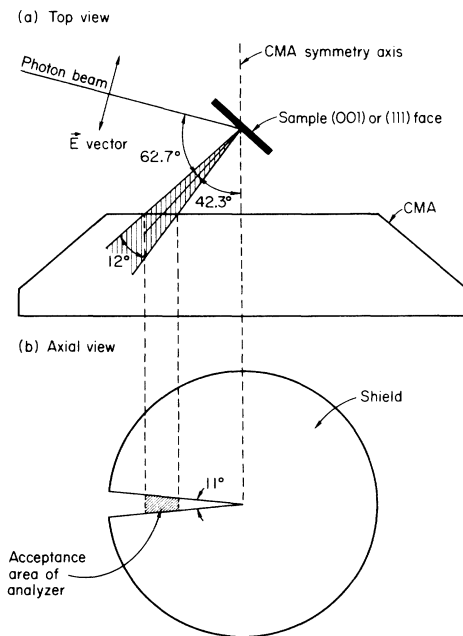vertical plane (cf. Fig. 1). It was found that the

FIG. 1. Experimental geometry for angle resolved
photoemission studies of Cu and Au single crystals. A
cylindrical-mirror analyzer (CMA) is modified by means
of a slit aperture (shield) to allow angle resolved mea-
surements. The effective angular resolution is ±6° in
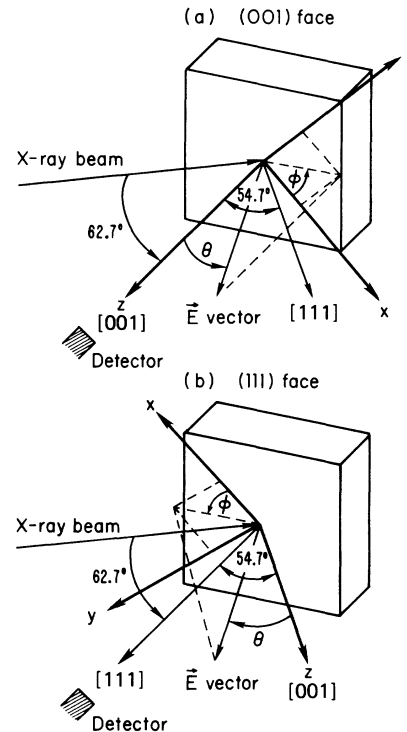the horizontal and ~±4° in the vertical plane.

FIG. 2. Experimental orientation of the x-ray beam,
$\vec{E}$ vector, and detector relative to the fourfold cubic
crystalline axes x, y, z. The polar (θ) and azimuthal (ϕ)
angles define the orientation of the $\vec{E}$ vector in the coor-
dinate system x, y, z. The crystal could be rotated about
a vertical axis. The x-ray beam, $\vec{E}$ vector, and detector
positions were fixed in a laboratory frame of reference
and lay in the horizontal plane.

shield reduces the counting efficiency of the CMA by approximately $360°/11°$, as expected. The Cu PED's were recorded at a pass energy (E_p) of 10 eV, except for the $\hbar\omega = 200$-eV spectra which were measured with $E_p = 15$ eV for Cu [001] and $E_p = 25$ eV for Cu [111]. The Au spectra were obtained with $E_p = 50$ eV. At a given pass energy the CMA used in the present study had an energy resolution of $\Delta E = 0.016\ E_p$ when operated without the slit aperture. It was found that the slit aperture improves the energy resolution of the analyzer. Measurements of core levels with and without the slit aperture showed that the resolution improves by approximately a factor of 2 when the aperture was used.[17] We thus believe that the Cu and Au spectra were recorded with a CMA resolution of $\Delta E < 0.15$ eV and $\Delta E \approx 0.4$ eV, respectively.

The angle-resolved experiments presented here were carried out in the photon energy range $32 \leqslant h\nu \leqslant 200$ eV for Cu and $32 \leqslant h\nu \leqslant 130$ eV for Au. The lower experimental limit (32 eV) is given by the possible mechanical motions of the monochromator.[13] The upper limit for Cu is given by the *resolution*[18] of the monochromator. We recorded Cu spectra up to $h\nu = 280$ eV [for even higher energies the absorption of carbon (K edge) on the various mirror surfaces resulted in a considerable decrease in *intensity*], but above $h\nu \approx 200$ eV the resolution decreases considerably and no difference in the PED's for Cu [001] and Cu [111] could be observed.[18] The upper limit ($h\nu = 130$ eV) for Au was determined by the small Au $5d$ cross section at higher energies as will be discussed in more detail below. The low $5d$ cross section was also the reason for recording the Au PED's at a higher CMA pass energy.

In order to obtain information on the cross-section variation of the $5d$ band in Au with photon energy we have measured the variation of the $5d$ intensity in the range $40 \leqslant h\nu \leqslant 190$ eV. These studies were carried out with a resolution $\Delta E = 1.6$ eV $(E_p = 100$ eV). No aperture was used in order to average over various angles of electron emission and in order to improve the signal. The Au sample was a polycrystalline foil which was cleaned by argon ion bombardment and subsequently annealed by heating with an electron gun to remove surface damage.

III. RESULTS

A. Cu

Experimental results for Cu are shown in Fig. 3. For both crystal faces the electrons were taken off along the surface normals of the (001) and (111) faces as shown in Fig. 2. The experimental orientations are summarized in Table I. The spectra
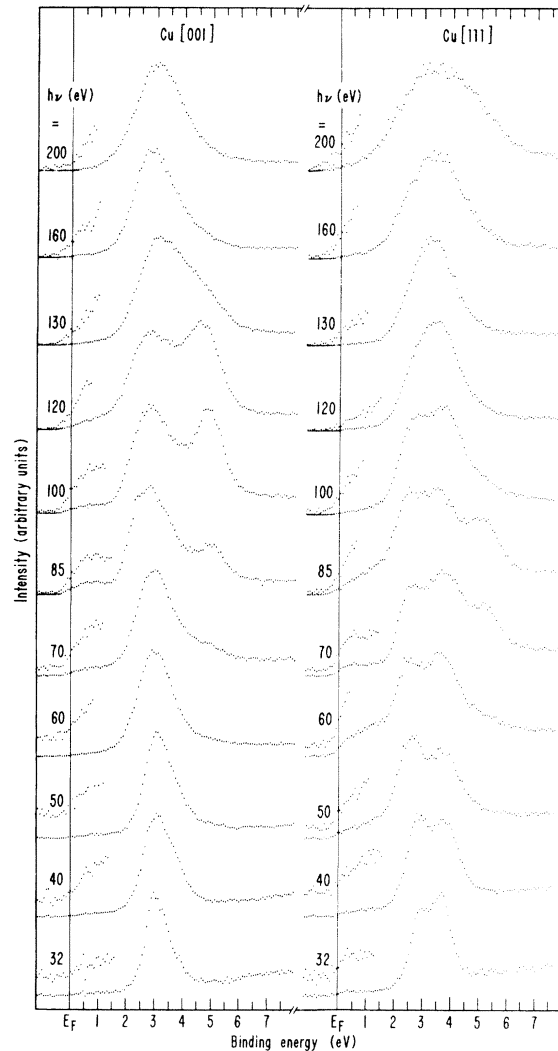

FIG. 3. Photoemission energy distributions from Cu single crystals in the range $32 \leq h\nu \leq 200$ eV. The Cu [001] and Cu [111] spectra were obtained by taking electrons off normal to the (001) and (111) single-crystal faces (compare Figs. 1 and 2 and Table I). The spectra are also shown enlarged around the Fermi energy.

are shown expanded around the Fermi energy, because the onset of photoemission is often very weak for Cu.

Several distinct trends are apparent in the PED's shown in Fig. 3. The $4s$ band, between the Fermi energy and 2-eV binding energy (BE), is strongest in the range 70–120 eV for Cu [001] and 60–85 eV for Cu [111]. Its strength, relative to the d-band intensity, is larger for Cu [111] than for Cu [001]. In Fig. 4 some PED's observed along the [001] and [111] directions are compared with each other. For all photon energies distinct differences are observed. Note that we have included some spectra ($h\nu = 80, 90, 110$ eV) in Fig. 4 which are not

TABLE I. Experimental geometry for photoemission from single crystals of Cu and Au.

	Cu[001] [b]	Cu[111] [b]	Au[001] [b]	Au[111] [b]
$\vec{E}$ vector [a]	$\theta = 27.5°$	$\theta = 27.5°$	$\theta = 27.5°$	$\theta = 30.0°$
	$\phi = 45°$	$\phi = 45°$	$\phi = 60.0°$	$\phi = 26.5°$
Detector [a]	$\theta = 0°$	$\theta = 54.5°$	$\theta = 0°$	$\theta = 54.5°$
	(along z axis)	$\phi = 45°$	(along z axis)	$\phi = 45°$

[a] All values have been rounded to the nearest 0.5°.
[b] Electrons were taken off normal to the (001) and (111) crystal faces, respectively.

shown in Fig. 3. The d band extends from ~2 eV to ~6 eV BE. For Cu [001], the most striking changes occur in the range $70 \leqslant \hbar\omega \leqslant 130$ eV. A feature at ~5 eV BE shows a broad resonance in intensity, peaking near $\hbar\omega = 110$ eV (compare Figs. 3 and 4). The PED's for Cu [111] exhibit a similar
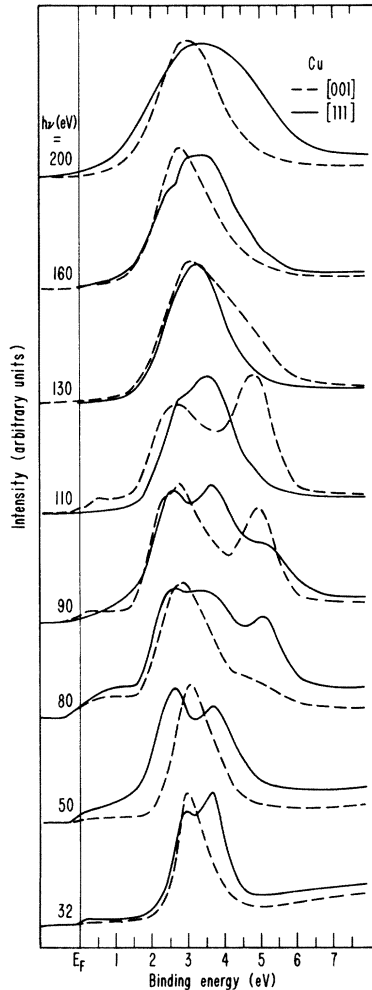

FIG. 4. Comparison of photoemission spectra taken along the Cu [001] and [111] directions (dashed and solid lines, respectively) for various photon energies. The experimental geometry was the same as for Fig. 3.

resonance in intensity of a peak at ~5-eV BE in the range $60 \leqslant \hbar\omega \leqslant 100$ eV, with a maximum at $\hbar\omega \approx 80$ eV (compare Figs. 3 and 4). At the highest photon energy (200 eV) this feature appears again to increase in intensity.

Figure 5 demonstrates the sensitivity of the PED's to the experimental geometry at $h\nu = 120$ eV. The dashed line corresponds to a spectrum taken at normal take-off from the (001) face and is identical to the Cu [001] spectrum at $\hbar\omega = 120$ eV in Fig. 3. As seen from Table I or Fig. 2(a) this geometry corresponds to an angle $\theta = 27.5°$ between the $\vec{E}$ vector and the fourfold z axis. The PED shown as a dashed curve in Fig. 5 was obtained by merely rotating the (001) crystal by 4° about a vertical axis such that in this case $\theta = 23.5°$ [compare Fig. 2(a)]. The difference between the two spectra in Fig. 5 is quite striking and it represents the strongest angular variation observed in the studied photon energy range.

In Fig. 6 we compare PED's taken to $h\nu = 90$ eV along a special symmetry direction ([001] or [111]) from different crystal faces. Electrons were taken off along the [001] direction either normal to the (001) face ($\alpha = 90°$) or at a take-off angle $\alpha \approx 35°$ with respect to the (111) face (compare Fig. 2). In the latter case the sample holder was rotated by ~55° about a vertical axis and raised to place the
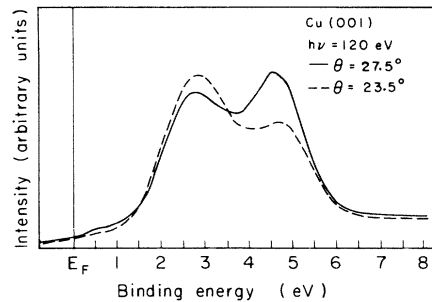

FIG. 5. Photoemission from a Cu (001) face at $h\nu = 120$ eV into the normal [001] direction ($\theta = 27.5°$) and into a direction 4° off the normal take-off direction ($\theta = 23.5°$). θ is defined in Fig. 2(a). In both cases $\phi = 45°$. The dashed spectrum corresponds to a detector orientation of $\theta_D = 4°$, $\phi_D = 225°$ in the frame x, y, z.
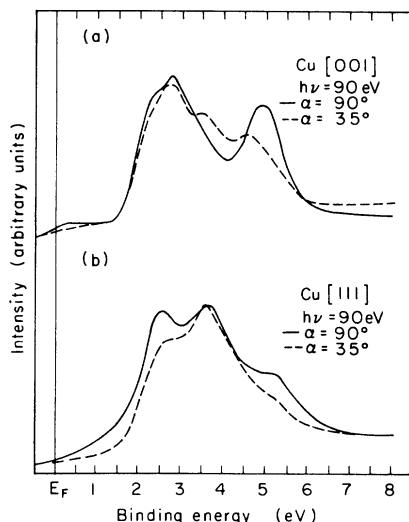
FIG. 6. (a) Comparison of photoemission spectra of Cu taken for electrons propagating along a [001] direction normal to a (001) crystal face ($\alpha = 90°$) and at a take-off angle of $\alpha = 35°$ from a (111) crystal face. The solid line corresponds to $\theta = 27.5°$ and $\varphi = 45°$ in Fig. 2(a), the dashed line to $\theta = 27.5°$, $\varphi = 225°$ in Fig. 2(b). (b) Spectra taken along a Cu [111] direction normal to a (111) crystal face ($\alpha = 90°$) and at a take-off angle of $\alpha = 35°$ from a (001) crystal face. The solid line corresponds to $\theta = 27.5°$, $\varphi = 45°$ in Fig. 2(b), the dashed line to $\theta = 82.5°$ and $\varphi = 45°$ in Fig. 2(a).

(111) crystal instead of the (001) crystal in the focal point of the x-ray beam and analyzer. Similarly, PED's were obtained for propagation along the [111] direction of the (111) crystal ($\alpha = 90°$) and the (001) crystal ($\alpha = 35°$). As seen from Fig. 6 there are distinct differences between the corresponding PED's of electron propagation. In both cases the spectra obtained at low take-off angles ($\alpha = 35°$) exhibit a narrowing in d-band width and increase in height at their center of gravity.

B. Au

PED's measured along the [001] and [111] directions from Au single crystals are shown in Fig. 7. The electrons were collected normal to the (001) and (111) faces, respectively. The experimental situation is shown in Fig. 2 and summarized in Table I. For both orientations the s band extending from the Fermi level to about 2-eV BE is most pronounced in the energy range 30–80 eV and loses intensity relative to the d-band peaks above 80 eV. The d band for Au consists of two main peaks centered around 3.5- and 6.5-eV BE. Both peaks can be approximately described as being composed of two components at ~3-eV and ~4-eV and ~6-eV and ~7-eV BE, respectively. The energy dependence of the PED's for both directions essentially con-
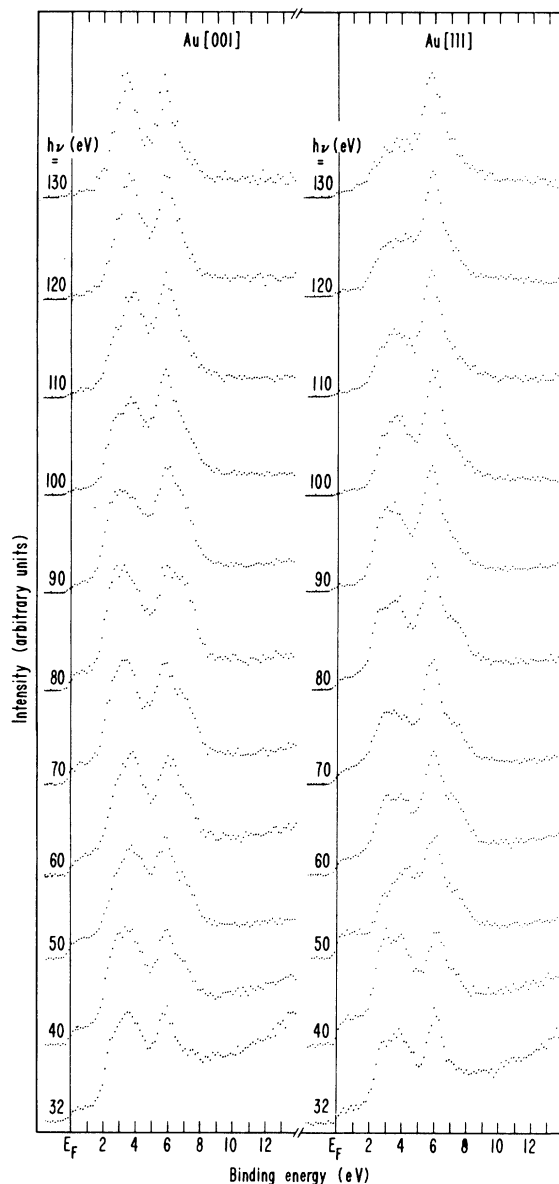

FIG. 7. Photoemission spectra from Au single crystals in the range $32 \leq h\nu \leq 130$ eV. The Au [001] and Au [111] spectra correspond to photoelectron propagation normal to the (001) and (111) single-crystal faces (cf. Figs. 1 and 2 and Table I).

sists of intensity changes of these four peaks. Spectra for electron emission into the [001] and [111] directions are compared in Fig. 8. As for the case of Cu, distinct changes between the two directions are observed.

The energy dependence of the Au $5d$ VB intensity in the range $40 \leq h\nu \leq 190$ eV is shown in Fig. 9 as a solid line. For comparison we have also included the Ag $4d$ VB photoemission intensity variation[12] in the figure. While the d-band intensity is given
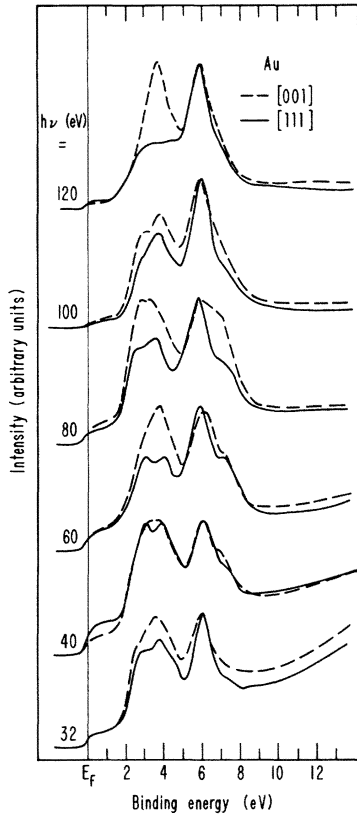
FIG. 8. Comparison of photoemission energy distributions along the [001] and [111] direction of Au (dashed and solid lines) in the range $32 \leq h\nu \leq 120$ eV. The spectra were taken from Fig. 7.

in arbitrary units, we have normalized the Ag $4d$ and Au $5d$ intensities to each other experimentally by comparing the areas under the PED's from Ag and Au at $h\nu = 40$ eV. The data points for Au shown in Fig. 9 were obtained by correcting the Au spectra for their inelastic background, measuring the
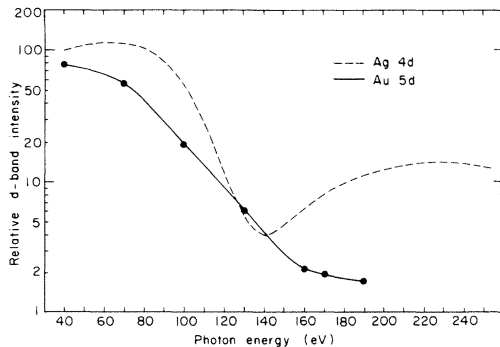

FIG. 9. Relative intensity of the $4d$ valence band of Ag (Ref. 12) and the $5d$ valence band of Au as a function of photon energy. The Ag and Au valence band intensities were normalized with respect to each other at $h\nu = 40$ eV.

area under the PED's in the binding energy range $2 \leq h\nu \leq 8$ eV, and correcting this area with respect to the incident photon flux and the collecting efficiency of the CMA.[12]

IV. GENERAL DISCUSSION OF ARP IN THE UPS-XPS TRANSITION REGION

In general, photoemission spectra depend on the details of the initial- (valence-band) and final- (conduction-band) state energies and wave functions. Analysis of experimental PED's thus requires the knowledge of these quantities. In the ultraviolet range ($h\nu \leq 40$ eV) photoemission spectra are usually analyzed by comparison with existing band-structure calculations assuming strict momentum and energy conservation in the excitation process. For example, ARP studies of[19] Cu and[20] Au at photon energies 16.8 and 21.2 eV were discussed in terms of the band-structure calculations by Janak *et al.*[21] and Christensen and Seraphin.[22] The interpretation of ARP spectra in the x-ray regime ($h\nu \geq 1000$ eV) is simplified by the fact that the details of the final-state band structure are unimportant. In this case certain approximations have been suggested which allow one to calculate the angle resolved PED's.[2,3] In the photon energy range covered in the present study, final-state band structure and transition-matrix-element effects are expected to be important. Because band-structure calculations are usually available[23] only to about 40 eV above the Fermi level the description of the final state is thus a major problem.

In a previous paper[11] on polycrystalline Cu we used a free-electron band structure and orthogonalized-plane-wave wave functions to describe the final state. However, in contrast to angle *integrated* photoemission from polycrystalline samples, angle *resolved* spectra from single crystals are far more sensitive to the exact nature of the final-state Bloch function. In a bulk interband optical transition an electron is ejected whose wave function

$$\psi_f(\vec{r}) = \sum_{\vec{G}} a_{\vec{G}} \exp[i(\vec{k}+\vec{G})\cdot\vec{r}] \tag{1}$$

has plane-wave components going in different directions $\vec{k}+\vec{G}$, where $\vec{G}$ is a reciprocal-lattice vector.[24] The intensity of emission into the direction $\vec{k}+\vec{G}$ is determined by the respective coefficients $a_{\vec{G}}$ in Eq. (1). By assuming free-electron final states all but the leading term in Eq. (1) are omitted and the electron may only leave in one direction. The resulting overemphasized angular anisotropies in the free-electron final-state picture are somewhat averaged out in angle-inte-

grated photoemission[11] but appear to preclude the prediction of ARP spectra.

In the intermediate photon energy range studied here another problem arises in the description of the final state. Because of strong inelastic scattering[8] the final-state wave function no longer represents a pure Bloch-wave characteristic of the bulk, but must include damping due to inelastic effects inside the solid. This may be accounted for in an *ad hoc* fashion by replacing the (surface) normal component of the wave vector in the final-state wave function by a complex quantity, which will exponentially favor emission from the surface layers.[25] The imaginary part then describes damping of the electron wave function inside the solid and may be related to the familiar mean free path.[26] In principle, with this *ad hoc* modification of the final-state wave function, the ARP spectra presented here could be analyzed by using a band-structure calculation which extends to higher energies. However, we feel that a more appropriate approach may be to calculate the photoemission spectra by using the multiple-scattering formalism[27] employed in current low-energy-electron-diffraction (LEED) theories.[28] Within this formalism, inelastic effects may be included by inserting a complex optical potential into the single-particle propagator.[29] Within the framework of the present paper no such calculation is attempted, but instead we discuss ARP in the UPS-XPS transition region in general terms and restrict the analysis of our experimental results to some basic observations.

At the intermediate photon energies used in the present study the changes in the PED's with *emission direction* are in part determined by the wave-vector dependence of the *final*-state energies and wave functions inside the crystal. In the following discussion we will assume that the angular distributions of photoelectrons is not affected by refraction at the crystal surface.[24] This is in general a good assumption if photoelectrons are studied along the normal of the sample. For photoemission along the [001] and [111] directions only final Bloch states which contain coefficients [cf. Eq. (1)] $a_{[00n]}$ ($n = 0, 2, 4, 6 \ldots$) and $a_{[mmm]}$ ($m = 0, 1, 2, 3 \ldots$), respectively, can contribute in a bulk photoemission process. Only these Bloch waves will have the correct propagation direction respectively, with their wave vectors $\vec{k} + \vec{G}$ pointing into the analyzer. Because of momentum conservation selection rules the nature of the final state also determines which *initial* states in the first Brillouin zone (BZ) are sampled. Even in the region of highest surface sensitivity, i.e., maximum broadening of the normal component of the photoelectron wave vector, the parallel

wave-vector components are conserved. For photoemission along a given symmetry line, only states in the first BZ along this line contribute.[30] The finite acceptance angle of the photoelectron analyzer results in sampling all initial states whose $\vec{k}$ vectors lie within a cone centered around the symmetry direction.[30] The cone diameter depends on the acceptance angle and photon energy, as discussed below.

The observed modulation effects in the PED's with *photon energy* arise mainly because of excitation into different final-state regions. In general, both the number of final states that satisfy energy and momentum conservation and the final-state Bloch functions (which determine the transition matrix element)[31] will change with photon energy. The number of final states increases with increasing photon energy and the leading coefficients in the Bloch functions [Eq. (1)] will correspond to larger reciprocal lattice vectors. For example, at $h\nu = 50$ eV photoemission along the [001] direction is strongly determined by the $a_{[002]}$ component of the final-state Bloch function [Eq. (1)], while the $a_{[004]}$ component is most important at $h\nu = 150$ eV.[32] The magnitude of the reciprocal lattice vector involved in the umklapp process of the final-state wave vector into the first BZ also determines how large a fraction of the first BZ (initial states) contributes to the ARP process. This is illustrated in Fig. 10(b) for photoemission into the [001] direction. We have as-
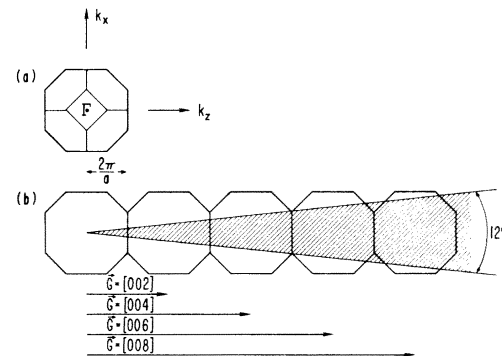

FIG. 10. (a) (010) projection of the three-dimensional Brillouin zone of a fcc lattice. The $\vec{k}$ axes are those of the infinite three-dimensional crystal. (b) Photoemission along the [001] direction assuming an angular resolution of ±6° (dashed area). The dashed area within the various zones indicates the fraction of initial states which may be sampled in the first Brillouin zone if the final state contain the respective $\vec{G}$ vector; i.e., these initial states are allowed by the *momentum* conservation selection rule. Whether they actually contribute to photoemission depends on satisfaction of the *energy* conservation selection rule imposed by the final-state band structure.

sumed a $\pm 6°$ acceptance angle of the analyzer
(dashed area), which is superimposed on the
(010) projection of the three-dimensional BZ of
the fcc lattice [compare Fig. 10(a)]. Depending
on the photon energy the final state will lie in
either the first, second, third, etc., BZ and
either the $\vec{G} = [000]$, $\vec{G} = [002]$, $\vec{G} = [004]$, etc., re-
ciprocal lattice vector will characterize the final
state. The complex final-state band structure in-
volving Bloch-type states (as opposed to free-elec-
tron final states) allows transitions with the prop-
er photoelectron propagation direction $\vec{k} + \vec{G}$ from
many points of the first BZ.[3] If the photoelectrons
are not refracted at the crystal-vacuum interface[24]
the dashed area in the respective BZ in Fig. 10(b)
is then exactly the part of the first BZ (initial
states) which may be sampled by means of an
umklapp process involving the corresponding $\vec{G}$
vector.

It is interesting to discuss what happens at high
photon energies; i.e., at XPS energies ($h\nu \gtrsim 1000$
eV). Here the number of final states is large and
a sufficient number of Bloch waves contain an ap-
propriate reciprocal lattice vector which reflects
the final state back into the first BZ by means of
an umklapp process. Because of the magnitude of
these vectors involved the whole first BZ is sam-
pled. The PED's are then determined by the
transition matrix element between the initial
states and the appropriate plane-wave components
of the final states [Eq. (1)]. As has been shown in
an earlier paper[3] photoemission along the [001]
and [111] directions samples the e_g and t_{2g} pro-
jections of the initial density of states, respective-
ly. After these general considerations, we shall
now be more specific and discuss some features
of the measured PED's for Cu and Au below.

V. DISCUSSION OF RESULTS

A. Cu

In contrast to the PED's from polycrystalline
Cu samples which did not show any significant
changes in spectral shape above $h\nu \approx 80$ eV,[11]
the spectra in Fig. 3 have not yet converged to
a constant shape even at $h\nu = 200$ eV. Note in
particular the opposite changes in width of the
d band for Cu [001] and Cu [111] in the range 130
$\leqslant h\nu \leqslant 200$ eV. These changes with photon energy
are thought to arise mainly from direct transi-
tions. It is somewhat surprising that the energy
dependence of the PED's is quite weak at the low-
est energies studied ($h\nu \leqslant 60$ eV). We have taken
additional spectra in the range $32 \leqslant h\nu \leqslant 40$ eV,
in increments of 2 eV, which showed a smooth
variation from the spectral shape at 32 eV to that at
40 eV shown in Fig. 3.

The region $70 \leqslant h\nu \leqslant 100$ eV is particularly in-
teresting, as the PED's for Cu [001] and Cu [111]
bear a close resemblence to the e_g and t_{2g} projec-
tions of the Cu $3d$ valence band. We have calcul-
ated the total density of states and its e_g and t_{2g}
projections using Smith's[33] parameterization of
the Hodges, Ehrenreich, and Lang[34] tight-binding
interpolation scheme. The results are shown in
Fig. 11. For Cu, a pronounced difference exists
between the e_g and t_{2g} projections, and ARP mea-
surements at XPS energies[35] for Cu [001] and Cu
[111] indeed show the spectral shapes predicted
by the above calculation. The question arises why
the d-band features around 85 eV resemble the
XPS results. From our previous results[11] on poly-
crystalline Cu and also from recent work on Au,[36]
there appears to be strong evidence that the min-
imum in escape depth for the noble metals Cu and
Au occurs around 90 eV. At first sight the re-
sulting momentum broadening in the final state,
which weakens final-state band-structure effects,[11]
appears to be a good candidate to explain the ob-
served PED's in the range around 85 eV. Let
us discuss this possibility in more detail.

At XPS energies the PED's obtained along the
[001] and [111] directions resemble the e_g and t_{2g}
projections of the valence band if two basic cri-
teria are fulfilled: (i) all initial states within the
first BZ are sampled; (ii) the transition matrix
element can be interpreted using plane-wave final
states.[3] At $h\nu = 85$ eV, photoemission from the
$bulk$, for example along the [001] direction, in-
volves final states with $\vec{G}$ vectors of the form
$[00n]$ with the $n = 2$ and $n = 4$ components dominating.
In this case photoemission into the $\Delta\Omega = \pm 6°$ ac-
ceptance cone of the analyzer dominantly derives
from initial states within the first BZ which cor-
respond to the dashed area in the second ($\vec{G} =
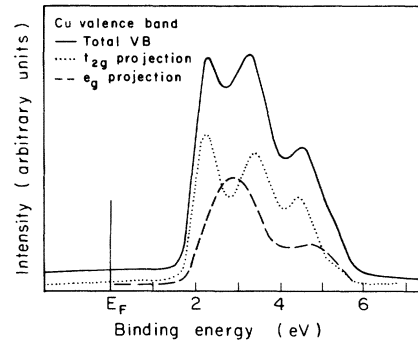= [002]$) and third ($\vec{G} = [004]$) zone in Fig. 10(b).[37]

FIG. 11. Total valence-band (VB) density of states and
the t_{2g} and e_g projections for Cu $3d$ calculated in a tight-
binding interpolation scheme as discussed in the text.
The density of states histograms were convoluted with a
Gaussian of full width at half-maximum of 0.5 eV.

As is seen from Fig. 10(b), all initial states which may contribute lie inside a cone centered along the k_z axis. At $h\nu = 85$ eV and $\Delta\Omega = \pm 6°$ only part of the three-dimensional first BZ is sampled. If the inelastic mean free path is small, the normal component of the final-state momentum vector becomes ill-defined because of a loss of (infinite) lattice periodicity near the surface in the normal direction. The problem of sampling the first BZ reduces to two dimensions (the $k_x - k_y$ plane). However, the area sampled in the $k_x - k_y$ plane does not increase by introducing momentum broadening in the k_z direction. Thus, although a relatively larger fraction of the first BZ is sampled in the momentum broadening case, an acceptance angle of $\pm 6°$ does not appear to be sufficient at $h\nu = 85$ eV to provide access to the whole $k_x - k_y$ plane. Even if we assume for the sake of argument that the most important parts of the first BZ are being sampled, the plane-wave description of the final state at such low photon energies still needs to be justified. On the basis of atomic considerations one would in general expect the interaction between the photoemitted electron and the ion-core potential to lead to more complicated (energy-dependent) angular distributions than those predicted by a plane-wave final state. For photoemission from d orbitals the angular distribution of the electrons is determined by the p and f partial-wave final-state channels. One important quantity which is a good indication of the strength of the interaction of the photoelectron and the ion-core, and hence of the validity of the plane-wave final-state description, is the phase shift.[38] Although we do not claim that the plane-wave final state description is valid for Cu at $h\nu = 85$ eV, we note that phase shifts for Cu are considerably smaller than for Au.[39] For this reason one would not expect to see the same energy and angular dependences for the Cu and Au PED's in the surface-sensitive region. The Cu spectra around 85 eV might resemble the t_{2g} and e_g projections because both criteria (i) and (ii) mentioned above are *approximately* satisfied.

One interesting question that arises in the intermediate photon energy regime concerns the effects of *surface* versus *bulk* photoemission. In general, surface sensitivity may be achieved if either the initial- or final-state wave-function is strongly localized at the surface. Such a situation is encountered for states at the surface whose energy corresponds to a band gap in the bulk.[1] Several studies in the ultraviolet regime of photoemission were concerned with the study of such *surface states* at clean metal surfaces.[40] For Cu, the existence of surface states has been postulated on experimental grounds by Gartland and Slags-

vold.[41] A peak of 0.4 eV below the Fermi level occurring in the PED's from Cu (111) at $h\nu \leqslant 6.6$ eV was interpreted as a surface band within the s-p band gap. A similar structure was also observed by Ilver and Nilsson[19] at $h\nu = 16.8$ eV. However, these authors pointed out an alternative explanation in terms of intraband excitations by the longitudinal component of the electric field at the surface.[42] Our experimental results do not provide any new information on the above problems, since in most cases the s band is quite weak and thus structures are not easily seen. For the d-band region of Cu no experimental evidence for surface states is available from previous photoemission studies.[40,43] A calculation for the (001) surface predicts a maximum in the density of surface states around 4.6 eV below the Fermi level.[43] The question arises whether the peak at ~5 eV BE which shows a broad resonance around 100 eV for Cu [001] corresponds to the calculated density of surface states. In lack of a detailed calculation this question cannot be answered unambiguously since the contributions from surface and bulk states to this peak cannot be separated. It is interesting to note the strong *angular* dependence of this peak as revealed by Fig. 5 at $h\nu = 120$ eV and by Fig. 6 at $h\nu = 90$ eV. The solid line in Fig. 6(a) corresponding to a take-off angle of $\alpha = 90°$ from a (001) face should be compared to the dashed curve in Fig. 6(b) which corresponds to $\alpha = 35°$ from the same (001) face {i.e., the [111] direction on the (001) face}. A similar strong enhancement of peak intensity in the direction normal to the crystal face as apparent from Figs. 5 and 6 has been observed for photoemission from surface states on W(001),[1] and Cu (111).[19,41]

Besides photoemission from surface states there has been considerable theoretical interest recently in studying the modification of bulk states near the surface.[44] The most interesting result of such calculations is the prediction of a narrowing of the d-band density of states near the surface.[44] In a simple physical picture such a behavior is expected because the reason for broadening atomic levels into solid-state bands is partly removed at the surface. We believe that we have observed this effect experimentally. As shown in Fig. 6 the experimental PED's along *both* the [001] and [111] directions become narrower when the take-off angle is changed from 90° to 35°. The above change in angle corresponds to a decrease in effective escape depth normal to the surface by a factor of 2.[45] Thus in the low take-off angle ($\alpha = 35°$) case the surface derived contribution to the spectrum is considerably enhanced. The fact that the escape depth is already short at $h\nu = 90$ eV[11,36] makes us believe that we are largely sam-

pling the outermost layer of the crystal in the low take-off angle case. The narrowing of the d-band width is accompanied by an increase of the central peak ($\sim$3.7 eV BE) which coincides with the center of gravity of the d band. This is expected because of increased atomic-type behavior at the surface.

B. Au

The photon energy dependence of photoemission from *polycrystalline* Au was studied by Freeouf et al.[46] in the range $15 \leq h\nu \leq 90$ eV. Above $h\nu \approx 40$ eV the spectral features in the observed PED's did not change significantly. This was discussed by Feibelman and Eastman[26] in terms of momentum broadening in the final state. Measurements by Lindau et al.[10] up to 200 eV revealed dramatic changes in the shape of the $5d$ valence band in the range above 100 eV. For example, the intensity ratio of the low ($\sim$3.5 eV BE) and high ($\sim$6.5-eV BE) peak decreased from a value of 1.5 at $h\nu = 100$ eV to 1.0 at $h\nu = 120$ eV. Lindau et al. discussed several possible explanations for the observed modulation effects and favored an explanation in terms of an atomic-type cross-section effect. In particular, they associated the two main VB peaks with the spin-orbit-split components $5d_{5/2}$ and $5d_{3/2}$ and argued that the respective cross sections may vary differently with photon energy. We can exclude this explanation on the basis of our experimental results.[47] An atomic-type cross section effect should also be seen in angle-resolved photoemission, i.e., in the range $100 \leq h\nu \leq 120$ eV for *both* Au [001] and Au [111]. Inspection of Fig. 7 or 8 reveals that is not the case for Au [001]. The above argument also excludes an atomic cross-section effect of the Cooper-Fano type[48] as being responsible for the observed modulation effect in Au. This is independently confirmed by the photon energy dependence of the total Au $5d$-band intensity (which is in good approximation proportional to the $5d$ cross section) shown in Fig. 9. In contrast to the case of the $4d$ intensity in Ag,[12,49] which exhibits a pronounced Cooper-minimum (cf. Fig. 9), the variation of the Au $5d$ intensity is not strong enough to significantly influence the shape of the valence band. We note that the PED's for Au [111] show a change in peak amplitudes for $100 \leq h\nu \leq 120$ eV (cf. Figs. 7 and 8) which goes in the same direction as those observed by Lindau et al.[10] In fact, the low BE peak decreases by a factor of 1.6 from $h\nu = 100$ eV to $h\nu = 120$ eV. Similar to the ARP results obtained for Cu, band-structure induced cross-section effects (i.e., final state plus matrix element effects) are thus found to be important for angle resolved photo-
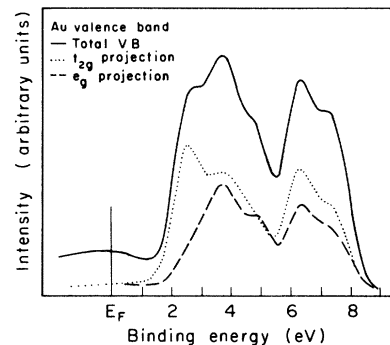

FIG. 12. Total valence-band (VB) density of states and the t_{2g} and e_g projections for the $5d$ band in Au. Calculations were carried out as for Fig. 11, with a spin-orbit coupling constant of 0.048 Ry included. A Gaussian of full width at half-maximum of 0.8 eV was used to convolute the density of states histograms.

emission from Au above 100 eV. In the light of the present results preferrential orientation of the crystallites in evaporated Au films may cause modulation effects similar to those observed in Ref. 10. In fact, such effects were observed for evaporated Au samples by Koyama and Hughey[50] at lower photon energies.

At the highest photon energies the Au spectra for photoemission along the [001] and [111] directions have not converged to the XPS limit[3] (also compare Fig. 12). Direct transition effects still appear to be important. In contrast to the case of Cu, the PED's for Au [001] and Au [111] do not reveal any resemblence to the e_g and t_{2g} projections of the initial density of states (cf. Fig. 12) in the surface sensitive energy range around 90 eV.[36] This finding does not necessarily lead to the conclusion that the resemblence of the ARP spectra for Cu with the initial-state projections is accidental in this energy range, but rather may imply that the case of Au is more complicated. Complications may arise from interference effects in the final state due to the photoelectron-ion core interaction[39] and the larger spin-orbit coupling.

VI. CONCLUSIONS

In this paper we have shown that, in contrast to angle-integrated photoemission measurements, ARP spectra have not converged to the XPS limit at the highest photon energies studied. This is attributed to the importance of direct transitions which restrict transitions to occur in only part of the BZ. In the case of Cu the PED's taken around $h\nu = 85$ eV along the [001] and [111] directions are found to resemble the e_g and t_{2g} projections of the initial $3d$ density of states, similar

to the spectra taken at XPS energies.[3,35] Momentum broadening in the final state due to a short inelastic mean free path in this energy region is discussed as a possible reason for such behavior. At $h\nu = 90$ eV a narrowing of the Cu PED's taken along equivalent symmetry directions is observed when the take-off angle is lowered from 90° to 35°. This is attributed to a preferential sampling the the surface local density of states by using an appropriate photon energy and a low take-off angle. For Au, the cross section of the $5d$ valence band has been measured as a function of photon energy. This is the first measurement of this kind for a $5d$ initial-state wave function. Furthermore we have presented new information on the modulation effects of the $5d$ valence-band peaks above $h\nu = 100$ eV, which were previously re-

ported for photoemission from polycrystalline Au.[10] We hope that the present experimental results will stimulate a detailed theoretical calculation, which may cast more light on the complex role of cross section versus surface effects in the transition region between UPS and XPS.

ACKNOWLEDGMENTS

*Work performed at the Stanford Synchrotron Radiation Project, which is supported by the NSF Grant No. DMR 73-07692 A02, in cooperation with the Stanford Linear Accelerator Center. The electron analyzer was purchased by funds obtained from NSF Grant No. GH-40132. This work was done with support from the U.S. Energy Research and Development Administration.

[1]For a recent review see B. Feuerbacher and R. F. Willis, J. Phys. C 9, 169 (1976).

[2]R. J. Baird, L. F. Wagner, and C. S. Fadley, in Faraday Discussion on Electron Spectroscopy of Solids and Surfaces, Vancouver, British Columbia, July, 1975 (unpublished); and Phys. Rev. Lett. 37, 111 (1976).

[3]F. R. McFeely, J. Stöhr, G. Apai, P. S. Wehner, and D. A. Shirley, Phys. Rev. B 14, 3273 (1976).

[4]See, for example, Ref. 1, pp. 182–185.

[5]For a recent review, see D. E. Eastman, in *Vacuum Ultraviolet Radiation Physics*, edited by E. E. Koch, R. Haensel, and C. Kunz (Pergamon, Vieweg, 1974), p. 417.

[6]H. Winick, in Ref. 5, p. 776.

[7]Synchrotron radiation experiments at SSRP are usually carried out in a parasitic mode on high-energy physics experiments. Typical electron beam currents are ~15 mA.

[8]I. Lindau and W. E. Spicer, J. Electron. Spectrosc. 3, 409 (1974); C. R. Brundle, Surf. Sci. 48, 99 (1975).

[9]C. Caroli, D. Lederer-Rozenblatt, B. Roulet, and D. Saint-James, Phys. Rev. B 8, 4552 (1973).

[10]I. Lindau, P. Pianetta, K. Y. Yu, and W. E. Spicer, Phys. Rev. B 13, 492 (1976).

[11]J. Stöhr, F. R. McFeely, G. Apai, P. S. Wehner, and D. A. Shirley, Phys. Rev. B 14, 4431 (1976).

[12]P. S. Wehner, J. Stöhr, G. Apai, F. R. McFeely, R. S. Williams, and D. A. Shirley, Phys. Rev. B 14, 2411 (1976).

[13]F. C. Brown, R. Z. Bachrach, S. B. M. Hagström, N. Lien, and C. H. Pruett, in Ref. 5, p. 785.

[14]P. W. Palmberg, J. Electron. Spectrosc. 5, 691 (1974).

[15]H. Niehus and E. Bauer, Rev. Sci. Instrum. 46, 1275 (1975). It should be noted that the CMA used in our

study (Phys. Electron.) does not accept electrons equally into its 360° acceptance cone. There are posts in four (1.5, 4.5, 7.5, and 10.5 o'clock) positions inside the analyzer which block the electrons along the respective trajectories. This fact has to be considered when rotating the slit for angle resolved studies as proposed in the above reference. In our case the slit was fixed in the 3 o'clock position and hence the posts had no effect on our measurements.

[16]The value $\Delta\alpha = 6°$ for the acceptance angle of the CMA quoted in Ref. 14 (footnote Fig. 1) is incorrect and should read $\Delta\alpha = 12°$ or $\alpha = (42.3 \pm 6)°$.

[17]These measurements were performed on the spin-orbit-split $4d_{3/2}$ and $4d_{5/2}$ doublet of indium.

[18]Assuming a constant band pass of 0.1 Å (Ref. 13) the resolution of the monochromator is given by $\Delta E = 8 \times 10^{-6} (h\nu)^2$ where both ΔE and $h\nu$ are in units of eV. However, at higher photon energies $(h\nu > 200$ eV) imperfections in the gratings and in the reflecting mirror surfaces appeared to increase the resolution over the above value.

[19]L. Ilver and P. O. Nilsson, Solid State Commun. 18, 677 (1976).

[20]P. O. Nilsson and L. Ilver, Solid State Commun. 17, 667 (1975).

[21]J. F. Janak, A. R. Williams, and V. L. Moruzzi, Phys. Rev. B 11, 1522 (1975).

[22]N. E. Christensen and B. O. Seraphin, Phys. Rev. B 4, 3321 (1971).

[23]We are aware of only one band-structure calculation extending above 100 eV, namely, for Al by V. Hoffstein and D. S. Boudreaux, Phys. Rev. B 2, 3013 (1970). Recently, a high-energy band structure of Au extending up to ~60 eV has been published by N. E. Christensen [Phys. Rev. B 13, 2698 (1976)].

[24]Following G. D. Mahan, Phys. Rev. B 2, 4334 (1970), the emission directions are often discussed in terms of "primary" and "secondary" cones.

[25]See for example the review article by J. W. Gadzuk, in *Electronic Structure and Reactivity of Metal Surfaces*, *NATO Advanced Study Institute Series* (Plenum, New

York, 1976).

[26]P. J. Feibelman and D. E. Eastman, Phys. Rev. B 10, 4932 (1974).

[27]A. Liebsch, Phys. Rev. B 13, 544 (1976).

[28]J. B. Pendry, Low Energy Electron Diffraction (Academic, New York, 1974); C. B. Duke, in Dynamic Aspects of Surface Physics, edited by F. O. Goodman (Editrice Compositori, Bologna, 1974), p. 99; D. W. Jepsen, P. M. Marcus, and F. Jona, Phys. Rev. B 5, 3933 (1972).

[29]R. O. Jones and J. A. Strozier, Phys. Rev. Lett. 22, 1186 (1969); C. B. Duke and C. W. Tucker, Phys. Rev. Lett. 23, 1163 (1969).

[30]Here we have neglected the photon wavevector. Also see R. F. Willis and B. Feuerbacher, Surf. Sci. 53, 144 (1975).

[31]In addition to matrix element effects which arise from the details of the band structure, atomic-type matrix element effects may be observed if the initial-state wave function has a radial node (Ref. 12).

[32]In order to estimate the most important $\vec{G}$ vector at a given photon energy one may use the free-electron relation $h\nu$ (eV) = $(12.26/a)^2(G_x^2 + G_y^2 + G_z^2)$, where a is the lattice constant in angstroms, and $|\vec{G}|$ is in units of $2\pi/a$.

[33]N. V. Smith, Phys. Rev. B 3, 1862 (1971).

[34]L. Hodges, H. Ehrenreich, and N. D. Lang, Phys. Rev. 152, 505 (1966).

[35]G. Apai, J. Stöhr, R. S. Williams, P. S. Wehner, S. P. Kowalczyk, and D. A. Shirley, Phys. Rev. B (to be published).

[36]I. Lindau, P. Pianetta, K. Y. Yu, and W. E. Spicer, J. Electron. Spectrosc. 8, 487 (1976).

[37]These states are allowed by the momentum conservation selection rule. Whether they actually contribute depends on satisfaction of the energy conservation selection rule.

[38]S. T. Manson, Phys. Rev. 182, 97 (1969).

[39]For p waves the phase shifts at threshold are 6.26 (Cu) and 12.40 (Au). For f waves the values are 0 (Cu) and 3.17 (Au) (compare Ref. 38).

[40]See Ref. 1, p. 203 ff.

[41]P. O. Gartland and B. J. Slagsvold, Phys. Rev. B 12, 4047 (1975).

[42]K. L. Kliewer, Phys. Rev. Lett. 33, 900 (1974).

[43]S. J. Gurman, Surf. Sci. 55, 93 (1976).

[44]For a review, see Ref. 1, p. 171–174 and pp. 203–211.

[45]W. A. Fraser, J. V. Florio, W. N. Delgass, and W. D. Robertson, Surf. Sci. 36, 661 (1973); C. S. Fadley, R. Baird, W. Siekhaus, T. Novakov, and S. A. L. Bergstrom, J. Electron. Spectrosc. 5, 725 (1975).

[46]J. Freeouf, M. Erbudak, and D. E. Eastman, Solid State Commun. 13, 771 (1973).

[47]Furthermore, we believe that the two Au $5d$ valence-band peaks cannot be discussed in terms of the two spin-orbit-split components $5d_{5/2}$ and $5d_{3/2}$ since solid-state effects are dominant.

[48]Such an effect has been observed for polycrystalline Ag. Compare Ref. 12 and references therein.

[49]We have measured some preliminary angle resolved PED's for Ag [001] and Ag [111] up to $h\nu = 130$ eV. These spectra also reveal the atomic cross-section effect discussed in Ref. 12.

[50]R. Y. Koyama and L. R. Hughey, Phys. Rev. Lett. 29, 1518 (1972).